Eur Radiol (2012) 22:2057–2066
DOI 10.1007/s00330-012-2479-1

PEDIATRIC

Accuracy, image quality and radiation dose comparison of high-pitch spiral and sequential acquisition on 128-slice dual-source CT angiography in children with congenital heart disease

Pei Nie · Ximing Wang · Zhaoping Cheng · Xiaopeng Ji · Yanhua Duan · Jiuhong Chen

Received: 7 January 2012 / Revised: 19 March 2012 / Accepted: 27 March 2012 / Published online: 18 May 2012

Abstract
Objectives To compare accuracy, image quality and radiation dose between high-pitch spiral and sequential modes on 128-slice dual-source computed tomographic (DSCT) angiography in children with congenital heart disease (CHD).
Methods Forty patients suspected with CHD underwent 128-slice DSCT angiography with high-pitch mode and sequential mode respectively. All the anomalies were confirmed by the surgical and/or the conventional cardiac angiography (CCA) findings. The diagnostic accuracy, the subjective and objective image quality and effective radiation doses were compared.
Results There was no significant difference in diagnostic accuracy (χ^2=0.963, P>0.05), the objective parameters for image quality (P>0.05) and the image quality of great vessels (u=167.500, P>0.05) between the two groups. The image quality of intracardiac structures and coronary arteries was significantly better in the sequential mode group than that in the high-pitch group (u=112.500 and 100.000, P<0.05). The mean effective dose in high-pitch group (0.17±0.05 mSv) was significantly lower (t=5.287, P<0.05) than that in the sequential mode group (0.29±0.09 mSv).
Conclusions Both the high-pitch and the sequential modes for 128-slice DSCT angiography provide high accuracy for the assessment of CHD in children, while the high-pitch mode, even with some image quality decrease, further significantly lowers the radiation dose.
Key Points
- *Modern CT provides excellent anatomical detail of congenital heart disease.*
- *Dual source CT systems offer high-pitch spiral and sequential modes.*
- *The high-pitch mode provides high accuracy for the assessment of CHD.*
- *A few images using the high-pitch mode were occasionally slightly degraded.*
- *But the high-pitch mode significantly lowers the radiation dose.*

Keywords Congenital heart disease · Dual source CT · High-pitch · Prospective ECG-triggering · Radiation exposure

P. Nie · X. Wang (✉) · Z. Cheng · X. Ji · Y. Duan
Shandong Provincial Key Laboratory of Diagnosis and Treatment of Cardio-cerebral Vascular Diseases, Shandong Medical Imaging Research Institute, Shandong University,
No.324, Jingwu Road,
Jinan, Shandong 250021, China
e-mail: wxming369@163.com

J. Chen
CT Research Collaboration, Siemens Ltd. China,
Beijing, China

Introduction

The recent rapid developments in multi-detector computed tomography (CT) have made it an important tool in the assessment of congenital heart disease (CHD) in children [1–4]. Non-ECG-gated spiral CT is widely used for the evaluation of thoracic and cardiovascular deformities in paediatric patients with CHD [1, 2, 5]. Even without ECG-gating, the origins and proximal segments of the coronary arteries are frequently observed [6]; however, visualisation of the coronary arteries was found to be age-dependent and heart-rate-dependent [7]. Electrocardiography (ECG)-gating should be applied for detailed assessment of coronary anatomy and intracardiac structures. Retrospective ECG-gated

CT is associated with relatively high radiation dose for its low pitch and overlapping data acquisition. Although the integration of the dose-saving features of heart rate adaptive pitch and ECG-controlled tube-current modulation can reduce the effective dose to 2–7 mSv for patients with CHD [8], high radiation dose is still the major limitation for retrospective ECG-gated CT. The radiation dose in ECG-gated angiography can be reduced substantially by performing prospective ECG-triggering sequential CT in paediatric patients [9–15]. The "Step-and-Shoot" (SAS) mode for dose reduction is characterised by administering maximum tube current at a predefined time points of the cardiac cycle; and this technique can reduce effective radiation dose to 0.2-0.7 mSv in newborns and infants [8].

Recently, the second generation dual-source CT (DSCT) system (Definition Flash, Siemens Healthcare, Forchheim, Germany) equipped with two 128-slice acquisition detectors has provided a high-pitch spiral mode. In this mode, data acquisition is also prospectively triggered with the ECG. With a very high pitch of 3.4 and fast table speed of 460 mm/s, the entire volumetric data acquisition can be completed within one single cardiac cycle [16, 17]. The radiation dose was consequently reduced due to the fast, non-overlapping spiral data acquisition. Recent studies have found that the new prospectively ECG-triggered high-pitch mode is feasible in adults with stable and low heart rates below 65 beats per minute (bpm) or 70 bpm with an effective dose of less than 1 mSv [18–24]. Goetti et al. [25] reported that a systolic acquisition window for high-pitch dual-source CT angiography in patients with high heart rates (≥70 bpm) significantly improves the image quality of coronary arteries; therefore, potential application of high-pitch mode in paediatric patients with higher heart rates has become possible. The study of Han et al. [26] demonstrated the feasibility and accuracy of high-pitch CT imaging in young children with CHD.

To the best of our knowledge, no study had been done on the evaluation and comparison of the performances of high-pitch mode and sequential mode with 128-slice DSCT. Thus, the purpose of this study was to compare the diagnostic accuracy, image quality and radiation dose of 128-slice DSCT angiography in children with CHD by two different protocols: a prospective ECG-triggered high-pitch spiral (high-pitch mode) and a prospective ECG-triggering sequential data acquisition (sequential mode).

Materials and methods

Patients

This study received approval from our institutional review board and written informed consent was obtained from the parents of all patients.

Forty consecutive patients suspected with CHD referred for DSCT examinations in our institution were enrolled in this study. Twenty patients (mean age: 11.00±11.43 months, age range: 1–48 months) underwent DSCT angiography using high-pitch spiral data acquisition (high-pitch mode), and the other 20 patients (mean age: 10.25±8.49 months, age range: 1–30 months) were examined using prospective ECG-triggering DSCT (sequential mode). Exclusion criteria were nephropathy or hypersensitivity to iodinated contrast medium. Except for surgery, conventional cardiac angiography (CCA) is usually recognised as the "gold standard" for diagnosing CHD [1, 27]. All the anomalies were confirmed by the surgical and/or the conventional cardiac angiography (CCA) findings. Surgery was performed in 27 patients, and CCA was performed in 15 patients.

DSCT protocol

All examinations were performed on a second generation DSCT scanner (Somatom Definition Flash, Siemens Healthcare, Forchheim, Germany). All patients were free-breathing. Short-term sedation was achieved with oral administration of chloral hydrate under the supervision of a paediatrician. Anaesthesia was not performed. The scans were performed in cranio-caudal direction from the aortic arch to the bottom of the heart.

CT parameters were as follows: 028 s gantry rotation time, 2×64×0.6 mm detector collimation, a slice collimation 2×128×0.6 mm by z-flying focal spot technique, 80 kV tube voltage and weight adapted setting for tube current (60 mAs/rotation for patients <5 kg body weight, 60–79 mAs/rotation for patients 5–10 kg body weight, 80–120 mAs/rotation for patients >10 kg body weight). In the high-pitch mode, data acquisition was prospectively ECG-triggered, starting at 10 % of the R-R interval using a pitch of 3.4. In the sequential mode, the acquisition window was set at 40-40 % of the R-R interval.

Iodinated contrast medium (Schering Ultravist, Iopromide, 350 mg I/ml, Berlin, Germany) was injected via peripheral veins at a volume of 1.5 ml/kg body weight with a saline chaser of 1.0 ml/kg body weight. The delay between the start of injection and the start of data acquisition was set at 25 s. Injection rate was calculated as the total injected volume divided by 25 s. For example, an 8-kg baby with peripheral access would be injected with 12 ml contrast medium and 8 ml saline at 0.8 ml/s.

DSCT data post-processing and analysis

Images were reconstructed with a slice thickness of 0.75 mm and increment of 0.5 mm using a medium smooth-tissue convolution kernel (B26f). All images were anonymous and transferred to an external workstation

(Multiple Modality Workplace, Siemens Healthcare, Forchheim, Germany) for further analysis. Multiplanar reformation (MPR), maximum intensity projection (MIP) and volume rendering (VR) were used for image interpretation.

Blinded to the results of surgical and/or CCA findings, two cardiac radiologists with more than 5 years' experience interpreted the image quality of intracardiac structures and great vessels using a five-grade scoring system (5, excellent; 4, good; 3, fair; 2, insufficient for complete evaluation; 1, not interpretable) [11]. The proximal and middle segments of coronary arteries were assessed using a five-grade scale (Grade 5, clear visualisation without any motion artefacts; Grade 4, mild motion artefacts, but still with high diagnostic confidence; Grade 3, obvious blurring; moderate diagnostic confidence; Grade 2, identified but equivocal, may simulate other structures; Grade 1, severe motion artefacts; no coronary segment visualised) [5]. The origins of the coronary arteries were included in the proximal segments. Grades 3, 4 and 5 were considered sufficient for complete diagnosis. For any disagreement in data assessment between the two observers, consensus agreement was achieved.

To assess the image quality objectively, the noise and signal-to-noise ratio (SNR) in the ascending aorta and the pulmonary trunk were measured by one observer who was not involved in the subjective image quality evaluation. Attenuation was measured in the middle of the ascending aorta and the pulmonary trunk in a 1-cm^2 circular region of interest (ROI) on the 0.75-mm-thick axial images. The noise was defined as the standard deviation of the attenuation value, and the SNR was calculated as the ratio of the attenuation value and the noise.

Radiation dose estimations

The volume CT dose index (CTDIvol) and dose-length product (DLP) were obtained from the information generated by the CT system and the effective radiation dose (mSv) was calculated from the DLP (mGy·cm) multiplied by 2.3 to adapt it to the 16-cm phantom (the DLP for the body surface area was given for a 32-cm phantom on the scanner protocol and the conversion factor of 2.3 is scanner specific for paediatric examinations at 80 kV as provided by the manufacturer). The corrected DLP value was then multiplied by the infant-specific conversion coefficients given for a 16-cm phantom: 0.039 mSv/[mGy·cm] for children up to 4 months, 0.026 mSv/[mGy·cm] between 4 months and 1 year of age, and 0.018 mSv/[mGy·cm] between 1 year and 6 years of age [11, 13, 15].

Statistics

Statistical analysis was performed by SPSS 17.0 software (SPSS, Chicago, IL, USA). Results were expressed as means ± standard deviations for quantitative variables and as frequencies or percentages for categorical variables. With surgical and/or CCA results as the standard, the diagnostic accuracy for the separate cardiovascular abnormalities was evaluated. Comparative analysis of the diagnostic performances between the high-pitch spiral mode and the sequential mode was obtained by non-parametric chi–squared test. The image quality scores were compared by using the Mann–Whitney *U* test. Interobserver agreement on grades of image quality was assessed by kappa statistics ($\kappa > 0.81$, excellent agreement; $\kappa = 0.61$-0.80, good agreement). The Student's *t*-test was performed to analyse the differences between the two groups regarding patient demographics, image noise, SNR and radiation dose. $P < 0.05$ was considered statistically significant.

Results

Patient demographics

All 40 patients underwent successful scanning with either high-pitch spiral mode or sequential acquisition. The male patients in the high-pitch group and sequential acquisition group were 13 (65 %) and 14 (70 %) respectively. Patients were adequately matched regarding to the mean age ($t = 0.236$, $P > 0.05$), mean body weight ($t = 0.128$, $P > 0.05$) and mean heart rate ($t = 0.565$, $P > 0.05$) during scan. The patient demographics are given in Table 1.

Diagnostic accuracy

Using surgical and/or CCA findings as the reference standard, a total of 71 and 69 separate cardiovascular anomalies were confirmed in the high-pitch group and sequential acquisition group, respectively. Table 2 demonstrates the details on separate cardiovascular abnormalities. Four cases

Table 1 Patient demographics of high-pitch mode and sequential mode on 128-slice DSCT angiography

Demographics	High-pitch mode $n=20$	Sequential mode $n=20$	t	P
Mean age (months)	11.00±11.43	10.25±8.49	0.236	0.815
Mean body weight (kg)	7.75±2.40	7.65±2.54	0.128	0.899
Mean heart rate during scan (bpm)	123.20±14.76	120.60±14.33	0.565	0.575
Mean acquisition time (s)	0.25±0.02	2.43±0.79	12.263	0.000

Table 2 Findings at 128-slice DSCT high-pitch mode (n=20) and sequential mode (n=20) referring to surgical and/or conventional cardiac angiography (CCA) results

Cardiovascular deformities	High-pitch group					Sequential scanning group				
	Surgical/CCA results	TP	TN	FP	FN	Surgical/CCA results	TP	TN	FP	FN
Atrial septal defect	5	4	14	1	1	6	5	13	1	1
Ventricular septal defect	12	12	8	0	0	14	14	6	0	0
Right ventricular outflow tract stenosis	2	2	18	0	0	6	6	14	0	0
Double outlet right ventricle	1	1	19	0	0	2	2	18	0	0
Pulmonary artery atresia	4	3	16	0	1	2	2	18	0	0
Pulmonary artery stenosis	3	3	17	0	0	4	4	16	0	0
Dilated pulmonary artery	6	6	14	0	0	1	1	19	0	0
Anomalous origin of pulmonary artery	1	1	19	0	0	1	1	19	0	0
Anomalous pulmonary venous return	1	1	19	0	0	-	-	-	-	-
Patent ductus arteriosus	10	9	10	0	1	3	3	17	0	0
Overriding aorta	4	4	16	0	0	7	7	13	0	0
Coarctation of the aorta	6	6	14	0	0	4	4	16	0	0
Interrupted aortic arch	1	1	19	0	0	-	-	-	-	-
Right aortic arch	4	4	16	0	0	4	4	16	0	0
Aortopulmonary window	1	1	19	0	0	-	-	-	-	-
Transposition of the great arteries	-	-	-	-	-	3	3	17	0	0
Major aortopulmonary collateral artery	6	6	14	0	0	5	5	15	0	0
Mirror-image heart	-	-	-	-	-	1	1	19	0	0
Coronary artery anomaly	4	2	16	0	2	6	6	14	0	0
Total	71	66	268	1	5	69	68	250	1	1

TP true positive detection, *TN* true negative detection, *FP* false positive detection, *FN* false negative detection

of CHD are shown in Figs. 1, 2, 3, 4. The sensitivity, specificity, positive predictive value (PPV) and negative predictive value (NPV) were 92.96 %, 99.63 %, 98.51 % and 98.17 %, respectively for the high-pitch group, and 98.55 %, 99.60 %, 98.55 % and 99.60 %, respectively for the sequential acquisition group. The diagnostic accuracy of the high-pitch group and sequential group was 98.24 % (334/340) and 99.38 % (318/320) respectively. There was no significant difference in the diagnostic accuracy between the high-pitch group and sequential acquisition group (χ^2=

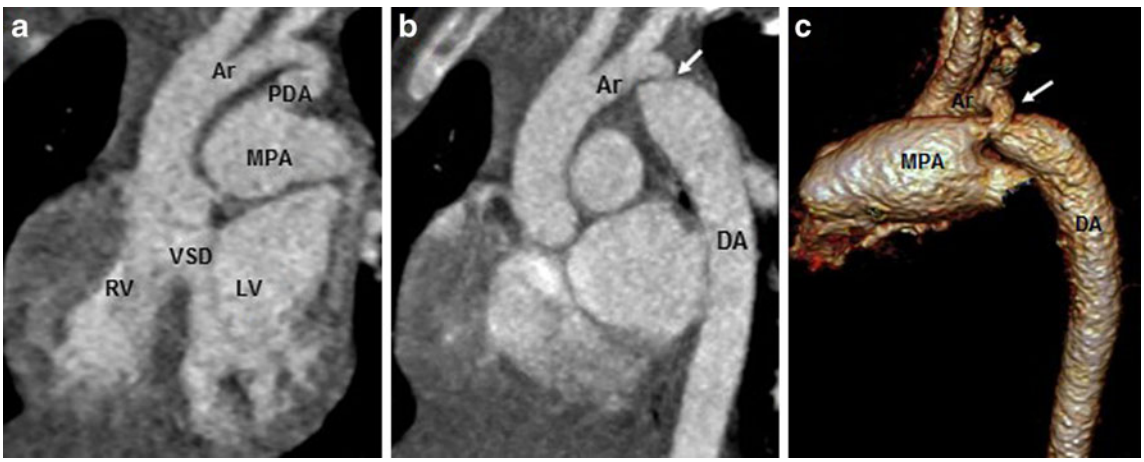

Fig. 1 A 13-month old boy with coarctation of the aorta. Prospective ECG-triggering high-pitch DSCT angiography was performed at 80 kV and 60 mAs/rotation (effective radiation dose, 0.12 mSv). **a** Thick-section oblique sagittal MIP shows ventricular septal defect (*VSD*) and patent ductus arteriosus (*PDA*) between aortic arch (*Ar*) and main pulmonary artery (*MPA*). **b** Thick-section oblique sagittal MIP and **c** volume-rendered image show coarctation of the aorta (*arrow*) and PDA. *RV* right ventricle, *LV* left ventricle, *DA* descending aorta

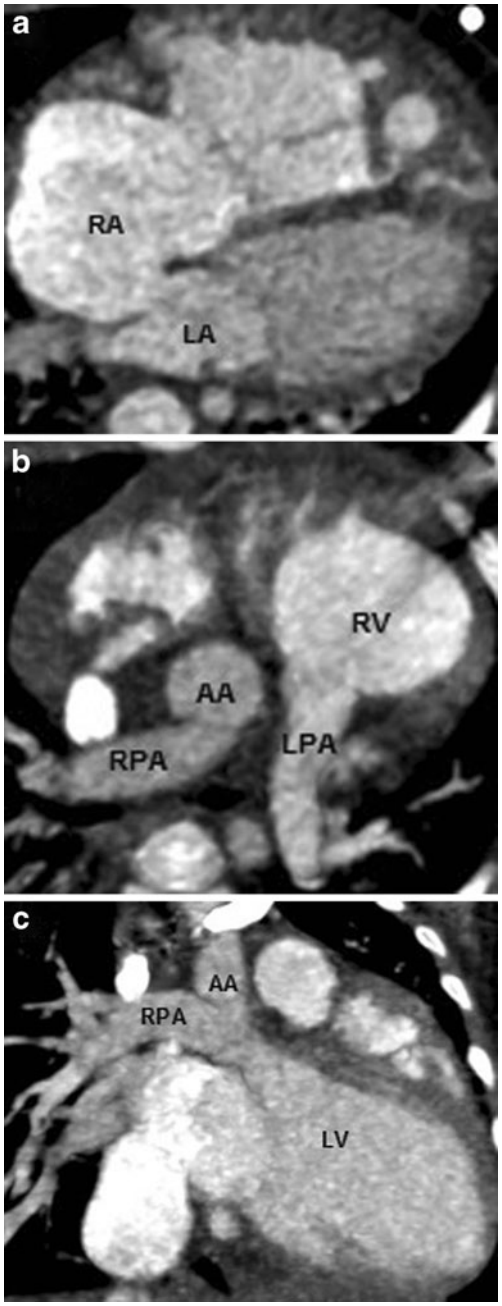

Fig. 2 A 5-month-old girl with the diagnosis of anomalous origin of the right pulmonary artery with atrial septal defect. Prospective ECG-triggering high-pitch DSCT angiography was performed at 80 kV and 60 mAs/rotation (effective radiation dose, 0.18 mSv). **a** Multiplanar reformatted image shows atrial septal defect (*ASD*). **b** Multiplanar reformatted image and **c** thick-section oblique coronal MIP show the right pulmonary artery arising from the ascending aorta (*AA*). *RA* right atrium, *LA* left atrium, *RPA* right pulmonary artery, *LPA* left pulmonary artery, *RV* right ventricle, *LV* left ventricle

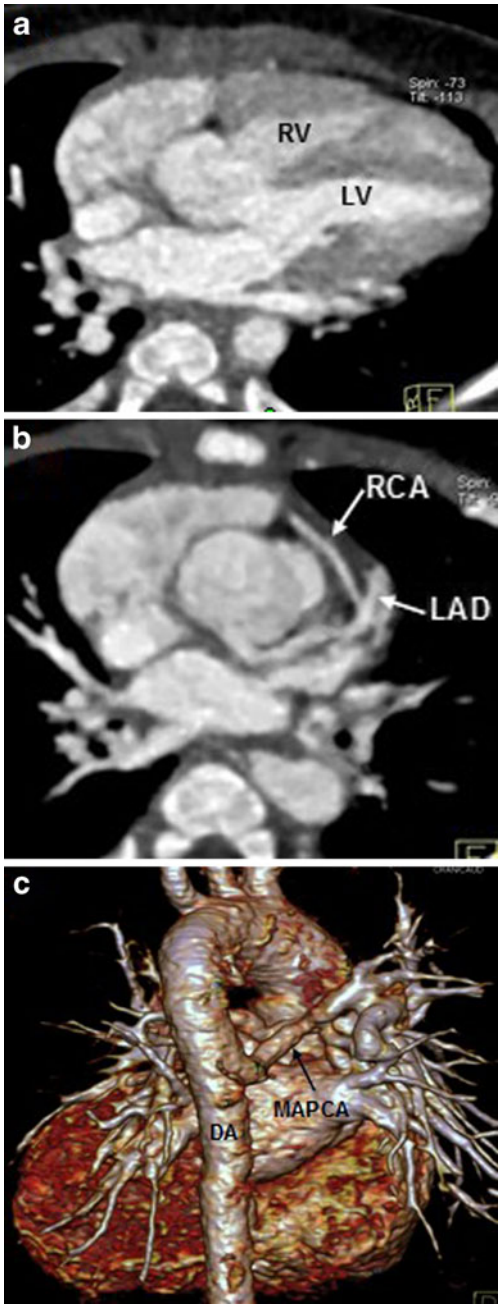

Fig. 3 A 4-month-old boy with the diagnosis of ventricular septal defect and coronary artery anomaly. The sequential DSCT angiography was performed at 80 kV and 60 mAs/rotation (effective radiation dose, 0.42 mSv). **a** MPR image shows ventricular septal defect (*VSD*). **b** MPR image shows anomalous RCA arose from the LAD. **c** Volume-rendered image (posterior view) shows a main aortopulmonary collateral artery (*MAPCA*) arising from the DA. *RV* right ventricle, *LV* left ventricle, *RCA* right coronary artery, *LAD* left anterior descending,, *DA* descending aorta

0.963, $P>0.05$, Table 3). Both high-pitch spiral and sequential CT data acquisitions failed to identify a small atrial septal defect and misdiagnosed another atrial septal defect as a normal variant. One case of pulmonary artery atresia and one case of patent ductus arteriosus were not identified by high-pitch mode. Coronary artery anomalies were missed in two patients (2/4) by high-pitch mode, whereas six cases (6/6) of coronary artery

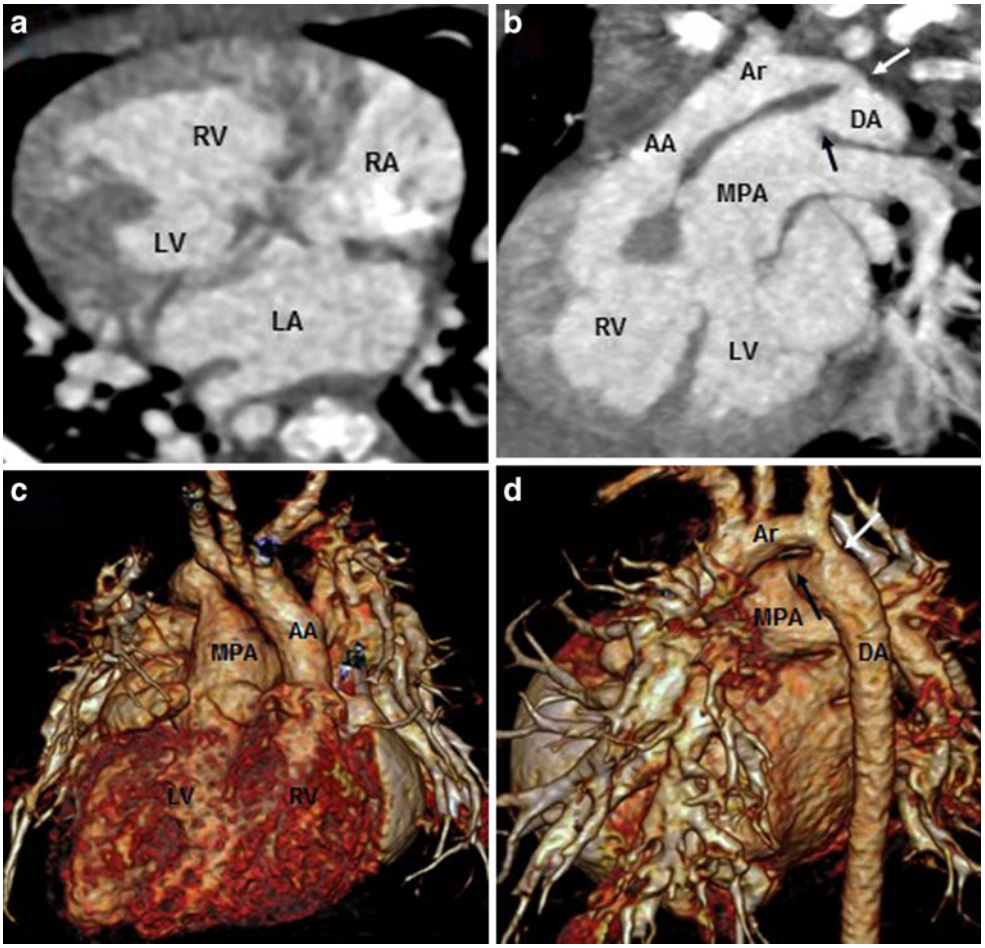

Fig. 4 Mirror-image heart with completed transposition of the great arteries in a 2-month-old girl. The sequential DSCT angiography was performed at 80 kV and 70 mAs/rotation (effective radiation dose, 0.63 mSv). **a** MPR image shows the mirror-image heart and atrial septal defect and ventricular septal defect (*VSD*). **b** Thick-section oblique sagittal MIP image and **c, d** volume-rendered images show transposition of the great arteries, VSD, patent ductus arteriosus (*PDA*, *black arrow*) and coarctation of the aorta (*white arrow*). *RV* right ventricle, *LV* left ventricle, *RA* right atrium, *LA* left atrium, *AA* ascending aorta, *Ar* aortic arch, *MPA* main pulmonary artery, *DA* descending aorta

anomalies were identified in sequential acquisition group.

Image quality assessment

Diagnostic images (images graded 3 or more) were obtained in sequential acquisition group. In the high-pitch group, the image scores of intracardiac structures and great vessels were 3 or more, but 30 % images (6/20) of proximal and middle segments of coronary arteries in high-pitch group were equivocal (images graded 2). The mean image quality score of intracardiac structures, great vessels and proximal and middle segments of coronary arteries were 4.05±0.76, 4.55±0.60 and 3.35±1.14, respectively by high-pitch spiral CT, and 4.65±0.49, 4.75±0.44 and 4.35±0.75, respectively by sequential CT. The agreement on the image quality scoring of the great vessels between the two observers was excellent (κ=0.84), and there was good agreement for the image quality scoring of the intracardiac structures (κ=0.79) and the proximal and middle coronary arteries (κ=0.79) between the two observers. There was no significant difference in the image quality of great vessels between high-pitch group and sequential acquisition group (u=167.500, P >0.05). The image quality of both intracardiac structures and the proximal and middle segments of coronary arteries was better in the sequential group than that in the high-pitch group (u=112.500 and 100.000, P<0.05).

The mean attenuation, the mean noise and the mean SNR in the ascending aorta and pulmonary trunk were 448.52±91.50 HU vs 458.02±88.78 HU, 18.04±5.48 HU vs 17.73±4.90 HU and 26.33±7.40 vs 27.86±9.96, respectively by the high-pitch group, and 434.15±93.77 HU vs 420.54±112.21 HU, 15.98±3.50 HU vs 15.37±3.57 HU and 28.08±

Table 3 Diagnostic performance of high-pitch mode and sequential mode on 128-slice DSCT angiography

Modality	Sensitivity	Specificity	PPV	NPV	Accuracy
High-pitch scan	92.96 %	99.63 %	98.51 %	98.17 %	98.24 %
Sequential scan	98.55 %	99.60 %	98.55 %	99.60 %	99.38 %

PPV positive predictive value, *NPV* negative predictive value

7.19 vs 27.98±6.13, respectively by the sequential group. There was no significant difference between the high-pitch group and the sequential group ($P>0.05$) regarding to the mean attenuation, the mean noise and the mean SNR in the ascending aorta and pulmonary trunk. The details of image quality evaluation are shown in Table 4.

Radiation dose estimation

There was a significant difference in the CTDIvol ($t=9.955$, $P<0.05$), DLP ($t=3.907$, $P<0.05$) and the effective radiation dose ($t=5.287$, $P<0.05$) between the high-pitch group and the sequential group. The mean CTDIvol of the high-pitch group and the sequential group was 0.27±0.08 mGy (range: 0.16-0.46 mGy) and 0.71±0.18 mGy (range: 0.41-1.14 mGy) respectively. The mean DLP of the two groups was 3.10±1.12 mGy·cm (range: 2-5 mGy·cm) and 5.10±2.00 mGy·cm (range: 3-11 mGy·cm), resulting in a mean estimated effective dose of 0.17±0.05 mSv (range: 0.08-0.27 mSv) and 0.29±0.09 mSv (range: 0.17-0.46 mSv). Radiation dose estimates are shown in Table 5.

Discussion

The second-generation DSCT is equipped with two independent X-ray tubes and two detectors arranged at an angular offset of 95°. Each detector enables data acquisition with 64 detector rows of 0.6 mm width, providing two sets of 128 overlapped 0.6-mm slices with the use of the z-flying focal spot. With a gantry rotation time of the system of 0.28 s, a quarter rotation for data reconstruction provides a temporal resolution of 75 ms in the centre of the field of view [16, 17]. Dual-source geometry and high temporal resolution enable the DSCT system to achieve a pitch value of up to 3.4 without reconstruction gap [28].

The innovation of second-generation DSCT has enabled high image quality in paediatric CT while constantly reducing radiation dose [11, 26, 29, 30]. Our study demonstrates that both the high-pitch mode and the sequential mode of 128-slice DSCT share a high diagnostic accuracy at low radiation dose. The accuracy of the high-pitch mode and the sequential mode in diagnosing cardiovascular deformities was 98.24 % and 99.38 % respectively. Although the image quality is mildly declined with the high-pitch mode, it further lowers the radiation dose to 0.17±0.05 mSv compared with the sequential mode.

Image quality

In high-pitch mode, data acquisition is completed in a single cardiac cycle with a time window of approximately 0.25 s. Heart rate is the key factor that influences the image quality of the high-pitch spiral acquisition. In this mode, ECG is used to trigger the start of the high-pitch data acquisition at a pre-selected phase of the patient's cardiac cycle. Since the table needs about 1 s for acceleration, the timing of at least two R-R intervals has to be prospectively estimated. Several studies have found that low and stable heart rates are essential in the high-pitch spiral mode [18–25, 28, 31–33]. Goetti et al. [25] recently found that with heart rates >70 bpm, the best acquisition window shifted to systole. Based on his results, the starting of the data acquisition was prospectively set at 10 % of the R-R interval in order to obtain a systolic acquisition window for the proximal and middle segments of coronary arteries. Heart rates of paediatric patients with CHD are always high and unstable. Irregular heart rates would lead to inaccurate starting positioning of the data acquisition, with data being acquired either too early or too late in the cardiac cycle [16–18, 24]. Therefore, somewhat inaccurate starting positioning of the acquisition occurred in 30 % (6/20) of patients with irregular heart rates, and led to unsatisfactory image quality (graded 2) of the proximal and middle segments of coronary arteries (Fig.5). Furthermore, the displaying of intracardiac structures was influenced to some extent as well. In our study, two cases of

Table 4 Subjective and objective image quality evaluation of high-pitch mode and sequential mode on 128-slice DSCT angiography

	High-pitch scan	Sequential scan	*u/t*	*P*
Mean image score of intracardic structures	4.05±0.76	4.65±0.49	$u=112.500$	0.009
Mean image score of great vessels	4.55±0.60	4.75±0.44	$u=167.500$	0.281
Mean image score of the proximal and middle segments of coronary arteries	3.35±1.14	4.35±0.75	$u=100.000$	0.005
Mean attenuation in the ascending aorta (HU)	448.52±91.50	434.15±93.77	$t=0.491$	0.672
Mean noise in the ascending aorta (HU)	18.04±5.48	15.98±3.50	$t=1.414$	0.165
Mean SNR in the ascending aorta	26.33±7.40	28.08±7.19	$t=0.758$	0.453
Mean attenuation in the pulmonary trunk (HU)	458.02±88.78	420.54±112.21	$t=1.172$	0.249
Mean noise in the pulmonary trunk (HU)	17.73±4.90	15.37±3.57	$t=1.744$	0.089
Mean SNR in the pulmonary trunk	27.86±9.96	27.98±6.13	$t=0.046$	0.964

Table 5 Radiation dose estimates of high-pitch mode and sequential mode on 128-slice DSCT angiography

	High-pitch scan	Sequential scan	*t*	*P*
Mean CTDIvol (mGy)	0.27±0.08	0.71±0.18	9.955	0.000
Mean DLP (mGy·cm)	3.10±1.12	5.10±2.00	3.907	0.000
Mean effective radiation dose (mSv)	0.17±0.05	0.29±0.09	5.287	0.000

coronary artery anomalies were not identified using high-pitch mode because of the poor image quality of the coronary arteries.

With prospective ECG-triggering DSCT in children with CHD, the best phase for reconstruction was reported to be end-systole [34]. In our experience, the data acquisition window setting at 40-40 % of R-R interval provides sufficient image quality in most cases. Compared with high-pitch mode, sequential mode may result in stair-step artefacts between adjacent slabs [11, 24]. Stair-step artefacts usually do not occur in high-pitch mode because the entire data acquisition is completed within a single cardiac cycle. Stair-step artefacts occurred in three patients in the sequential mode, but no such artefacts were seen when using the high-pitch. Motion artefacts occurred in one child in the sequential acquisition group because of the patient's movement.

To sum up, the high-pitch mode is recommended on the patient with a regular heart rate. Furthermore, when the primary indication of the CT study is to evaluate great vessels, the high-pitch mode would be a better choice regardless of the heart rate.

Radiation dose

Ait-Ali et al. [35] found that children with CHD were exposed to a significant cumulative dose that might lead to acute radiation-induced chromosomal DNA damage. The "ALARA" (as low as reasonable achievable) principle has to be considered thoroughly before each examination, especially in paediatric patients.

Several dose-saving strategies were performed in our study. Lowering tube voltage or tube current is the effective method for radiation dose reduction. The 80 kV setting is

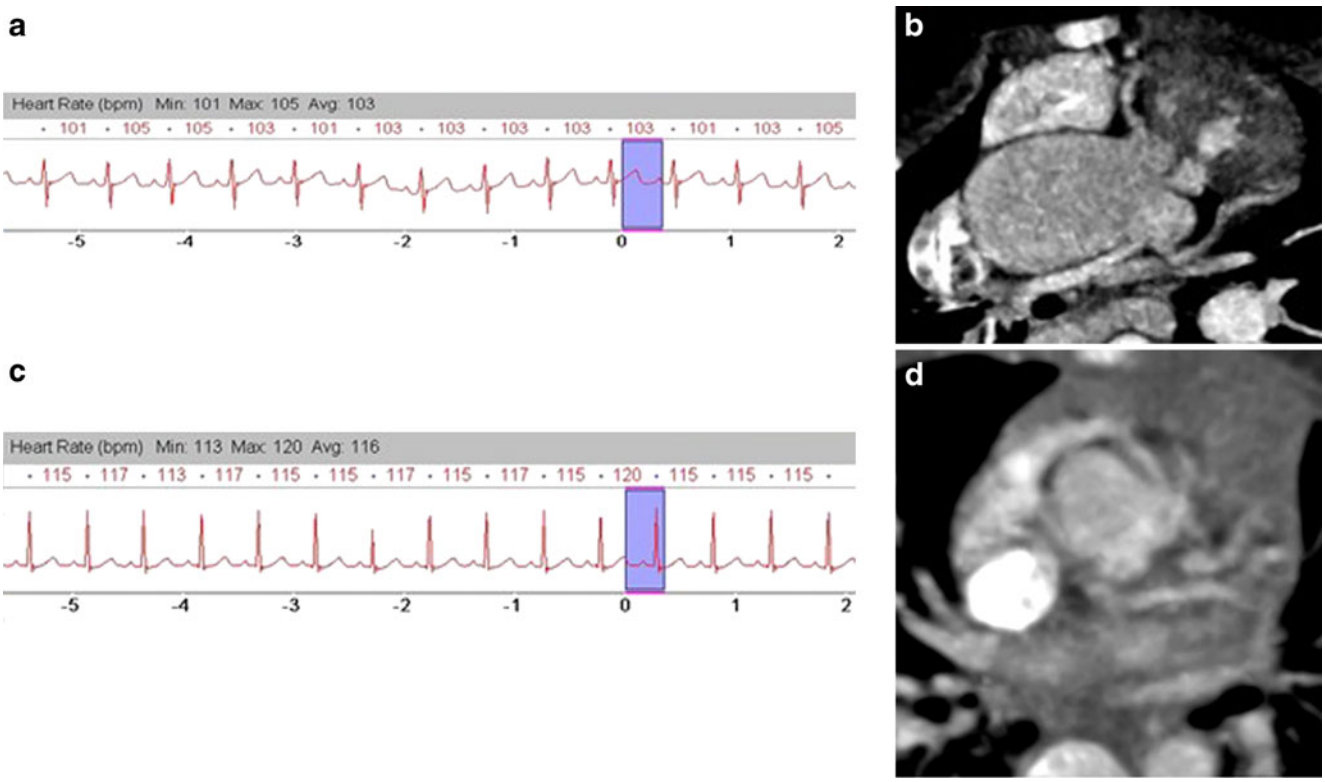

Fig. 5 High-pitch spiral DSCT for evaluation of coronary arteries with different HRs. The ECG signal (**a**) demonstrates a regular heart rate before data acquisition, and the starting phase was the pre-selected 10 % of the R-R interval leading to a satisfactory image quality of the proximal coronary arteries (**b**). The ECG signal (**c**) shows that the initial heart rate of 115 bpm increased to 120 bpm before acquisition, and phase acquisition was at 56–3 % of the R-R interval. Multiplanar reformatted image (**d**) demonstrates the non-diagnostic image quality of the proximal coronary arteries

now routinely for infants and small children CT examinations, and the adapted tube current to body weight is recommended [36]. In our study, the 80 kV tube setting along with the adaptation of the tube current to body weight drastically reduce the radiation dose. Even though the image noise increased as tube voltage decreased, none of our results approached 20 HU, which was previously published as an acceptable noise threshold in low-kilovoltage protocols [10]. In sequential mode, the data acquisition window setting at 40-40 % of R-R interval can reduce the radiation dose when compared with adaptive prospective ECG-triggering with a wider acquisition window. However, 46 % dose reduction was shown in the high-pitch spiral mode when compared with the sequential mode. The dose reduction was 25 % in the previous phantom study [16]. There are two main reasons why the high-pitch mode has a lower radiation dose compared with the sequential mode. First of all, the sequential technique needs an overlap of about 10 % between the individual axial image reconstructions because of the cone-beam geometry. This overlap is not needed for the high-pitch spiral mode. In addition, the sequential scan technique requires a "beam on" time corresponding to the minimum partial data interval for each axial image; whereas the high-pitch spiral requires the extra "beam on" time only once, at the beginning and at the end of the spiral acquisition. Thus, the cumulative "beam on" time is decreased for the high-pitch spiral technique [16].

Although transthoracic echocardiography is the first-line method for children with CHD, DSCT angiography is more effective in demonstrating extracardiac structures, such as the coronary arteries, the aorta, the pulmonary vessels and the significant aortopulmonary collateral vessels. Accurate assessment of these anomalies is of great importance before the thoracic surgeon. In this study, surgery was performed in 27 patients, our CT findings offered important information for the surgical strategies.

Limitations

Our study has some limitations. Firstly, a relatively small group of patients was included; future studies on the comparison of the high-pitch spiral mode and sequential acquisition mode on 128-slice DSCT with larger patient populations are required. Secondly, in high-pitch mode, the actual starting phase of data acquisition was not coordinated with the pre-selected starting phase in paediatric patients with high and irregular heart rates, leading to unsatisfactory image quality of the coronary arteries and intracardiac structures. This problem has not been solved and will be addressed in our future research. Last, the benefits of raw data-based iterative reconstruction approaches which have the potential to further reduce radiation dose were not assessed in this study.

In conclusion, both the high-pitch mode and the sequential mode for dual-source 128-slice CT allow high diagnostic accuracy in the assessment of CHD in children. The high-pitch mode, as compared with the sequential mode, further lowers the radiation dose even though the image quality was occasionally slightly lower.

References

1. Tsai IC, Chen MC, Jan SL et al (2008) Neonatal cardiac multidetector row CT: why and how we do it. Pediatr Radiol 38:438–451
2. Paul JF, Rohnean A, Sigal-Cinqualbre A (2010) Multidetector CT for congenital heart patients: what a paediatric radiologist should know. Pediatr Radiol 40:869–875
3. Krishnamurthy R (2009) The role of MRI and CT in congenital heart disease. Pediatr Radiol 39:S196–S204
4. Krishnamurthy R (2010) Neonatal cardiac imaging. Pediatr Radiol 40:518–527
5. Ben Saad M, Rohnean Aa, Sigal-Cinqualbre A, Adler G, Paul JF (2009) Evaluation of image quality and radiation dose of thoracic and coronary dual-source CT in 110 infants with congenital heart disease. Pediatr Radiol 39:668–676
6. Goo HW, Seo DM, Yun TJ et al (2009) Coronary artery anomalies and clinically important anatomy in patients with congenital heart disease: multislice CT findings. Pediatr Radiol 39:265–273
7. Young C, Taylor AM, Owens CM (2011) Paediatric cardiac computed tomography: a review of imaging techniques and radiation dose consideration. Eur Radiol 21:518–529
8. Goo HW (2010) State-of-the-art CT imaging techniques for congenital heart disease. Korean J Radiol 11:4–18
9. Jin KN, Park EA, Shin CI, Lee W, Chung JW, Park JH (2010) Retrospective versus prospective ECG-gated dual-source CT in paediatric patients with congenital heart diseases: comparison of image quality and radiation dose. Int J Cardiovasc Imaging 26:63–73
10. Kim JE, Newman B (2010) Evaluation of a Radiation Dose Reduction Strategy for Pediatric Chest CT. AJR Am J Roentgenol 194:1188–1193
11. Paul JF, Rohnean A, Elfassy E, Sigal-Cinqualbre A (2011) Radiation dose for thoracic and coronary step-and-shoot CT using a 128-slice dual-source machine in infants and small children with congenital heart disease. Pediatr Radiol 41:244–249
12. Huang MP, Liang CH, Zhao ZJ et al (2011) Evaluation of image quality and radiation dose at prospective ECG-triggered axial 256-slice multi-detector CT in infants with congenital heart disease. Pediatr Radiol 41:858–866
13. Pache G, Grohmann J, Bulla S et al (2011) Prospective electrocardiography-triggered CT angiography of the great thoracic vessels in infants and toddlers with congenital heart disease: feasibility and image quality. Eur J Radiol 80:e440–e445
14. Al-Mousily F, Shifrin RY, Fricker FJ, Feranec N, Quinn NS, Chandran A (2011) Use of 320-detector computed tomographic angiography for infants and young children with congenital heart disease. Pediatr Cardiol 32:426–432
15. Cheng Z, Wang X, Duan Y et al (2010) Low-dose prospective ECG-triggering dual-source CT angiography in infants and children with complex congenital heart disease: first experience. Eur Radiol 20:2503–2511
16. Flohr TG, Klotz E, Allmendinger T, Raupach R, Bruder H, Schmidt B (2010) Pushing the envelope: new computed tomography techniques for cardiothoracic imaging. J Thorac Imaging 25:100–111

17. Flohr TG, Leng S, Yu L et al (2009) Dual-source spiral CT with pitch up to 3.2 and 75 ms temporal resolution: image reconstruction and assessment of image quality. Med Phys 36:5641–5653
18. Lell M, Marwan M, Schepis T et al (2009) Prospectively ECG-triggered high-pitch spiral acquisition for coronary CT angiography using dual source CT: technique and initial experience. Eur Radiol 19:2576–2583
19. Wolf F, Leschka S, Loewe C et al (2010) Coronary artery stent imaging with 128-slice dual-source CT using high-pitch spiral acquisition in a cardiac phantom: comparison with the sequential and low-pitch spiral mode. Eur Radiol 20:2084–2091
20. Leschka S, Stolzmann P, Desbiolles L et al (2009) Diagnostic accuracy of high-pitch dual-source CT for the assessment of coronary stenoses: first experience. Eur Radiol 19:2896–2903
21. Achenbach S, Marwan M, Ropers D et al (2010) Coronary computed tomography angiography with a consistent dose below 1 mSv using prospectively electrocardiogram-triggered high-pitch spiral acquisition. Eur Heart J 31:340–346
22. Achenbach S, Goroll T, Seltmann M et al (2011) Detection of coronary artery stenoses by low-dose, prospectively ECG-triggered, high-pitch spiral coronary CT angiography. JACC Cardiovasc Imaging 4:328–337
23. Goetti R, Baumüller S, Feuchtner G et al (2010) High-pitch dual-source CT angiography of the thoracic and abdominal aorta: is simultaneous coronary artery assessment possible? AJR Am J Roentgenol 194:938–944
24. Alkadhi H, Stolzmann P, Desbiolles L et al (2010) Low-dose, 128-slice, dual-source CT coronary angiography: accuracy and radiation dose of the high-pitch and the step-and-shoot mode. Heart 96:933–938
25. Goetti R, Feuchtner G, Stolzmann P et al (2010) High-pitch dual-source CT coronary angiography: systolic data acquisition at high heart rates. Eur Radiol 20:2565–2571
26. Han BK, Lindberg J, Grant K, Schwartz RS, Lesser JR (2011) Accuracy and safety of high pitch computed tomography imaging in young children with complex congenital heart disease. Am J Cardiol 107:1541–1546
27. Lee T, Tsai IC, Fu YC et al (2006) Using multidetector-row CT in neonates with complex congenital heart disease to replace diagnostic cardiac catheterization for anatomical investigation: initial experiences in technical and clinical feasibility. Pediatr Radiol 36:1273–1282
28. Sommer WH, Albrecht E, Bamberg F et al (2010) Feasibility and radiation dose of high-pitch acquisition protocols in patients undergoing dual-source cardiac CT. AJR Am J Roentgenol 195:1306–1312
29. Lell MM, May M, Deak P et al (2011) High-pitch spiral computed tomography effect on image quality and radiation dose in pediatric chest computed tomography. Invest Radiol 46:116–123
30. Santiago-Herrera R, Ramirez-Carmona R, Criales-Vera S, Calderon-Colmenero J, Kimura-Hayama E (2011) Ectopia cordis with tetralogy of Fallot in an infant with pentalogy of Cantrell: high-pitch MDCT exam. Pediatr Radiol 41:925–929
31. Lell M, Hinkmann F, Anders K et al (2009) High-pitch electrocardiogram-Ttriggered computed tomography of the chest: initial results. Invest Radiol 44:728–733
32. Bamberg F, Marcus R, Sommer W et al (2011) Diagnostic image quality of a comprehensive high-pitch dual-spiral cardiothoracic CT protocol in patients with undifferentiated acute chest pain. Eur J Radiol. doi:10.1016/j.ejrad.2010.11.032
33. Sommer WH, Schenzle JC, Becker CR et al (2010) Saving dose in triple-rule-out computed tomography examination using a high-pitch dual spiral technique. Invest Radiol 45:64–71
34. Araoz PA, Kirsch J, Primak AN et al (2009) Optimal image reconstruction phase at low and high heart rates in dual-source CT coronary angiography. Int J Cardiovasc Imaging 25:837–845
35. Ait-Ali L, Andreassi MG, Foffa I, Spadoni I, Vano E, Picano E (2010) Cumulative patient effective dose and acute radiation-induced chromosomal DNA damage in children with congenital heart disease. Heart 96:269–274
36. Xu L, Zhang Z (2010) Coronary CT angiography with low radiation dose. Int J Cardiovasc Imaging 26:S17–S25